arXiv:1409.1438v1 [cond-mat.supr-con] 4 Sep 2014

Evidence of surface superconductivity and multi - quanta vortex states in a weakly - pinned single crystal of $Ca_3Ir_4Sn_{13}$

Santosh Kumar,[1,*] Ravi P. Singh,[2,†] A. Thamizhavel,[2] C. V. Tomy,[1] and A. K. Grover[2,3]

[1] *Department of Physics, Indian Institute of Technology Bombay, Mumbai 400076, India*
[2] *Department of Condensed Matter Physics and Materials Science, Tata Institute of Fundamental Research, Mumbai 400005, India.*
[3] *Department of Physics, Panjab University, Chandigarh 160014, India.*

Abstract

We report here the observation of anomalous paramagnetic signal(s) in the isofield field - cooled cool - down magnetization scans ($M_{FCC}(T)$) recorded for a single crystal of a low T_c superconductor $Ca_3Ir_4Sn_{13}$. Novel features emanating from the $M_{FCC}(T)$ response include an oscillatory magnetization behaviour below T_c and a rich multiplicity (non - uniqueness) in magnetization ranging from diamagnetism to paramagnetism at a given H, T value. The metastability in $M_{FCC}(T)$ has been ascribed to non - unique coexistence of multi - quanta vortex states ($L\Phi_0$, $\Phi_0 = hc/2e$, $L > 1$) and single quantum ($L = 1$, Abrikosov) vortices. Additionally, the isothermal $M(H)$ scans recorded across a short window of temperature just below T_c show evidence for only the multi - quanta vortex states in the domain of surface superconductivity, with no fingerprint(s) of pinned Abrikosov lattice.

PACS numbers: 74.25.Ha, 74.25.Op
Keywords: Paramagnetic response, surface superconductivity, multi-quanta states

I. INTRODUCTION

In recent years, the exploration of temperature variation of the field - cooled cool - down (FCC) magnetization ($M_{FCC}(T)$) measurements at low fields in a variety of superconductors [1–12] have revealed characteristics which have been ascribed to the phenomenon of surface superconductivity [13]. Many interesting features reported in the $M_{FCC}(T)$ responses at different fields in a weakly - pinned single crystal of a low T_c (~ 8.3 K) superconductor, $Ca_3Rh_4Sn_{13}$ [10], include the occurrence of anomalous paramagnetic magnetization *a la* paramagnetic Meissner effect (PME), modulations overriding PME like response, intersection of the $M_{FCC}(T)$ curves for different field values across a field interval at a characteristic temperature T^*_{VL}, below the onset temperature, T_c, of superconducting response, etc. Investigations in the low field regime in $Ca_3Rh_4Sn_{13}$ [10] had also revealed a concave curvature in the temperature dependence of the upper critical field line ($H_{c2}(T)$, $T_c(H)$) near its $T_c(0)$, which was conjectured to reflect the persistence of superconductivity at the surface [13] at low fields, up to third critical field H_{c3} values, which were well beyond the notional second critical fields, H_{c2}. The $T_c(H)$ values at low field were thus argued to represent the temperatures at which the superconductivity nucleated only on the surface, whereas the temperature T^*_{VL} was identified as the temperature below which the superconductivity permeated into the interior of the single crystal of $Ca_3Rh_4Sn_{13}$ [10].

We have recently explored [14] the vortex phase diagram in a single crystal of another low T_c superconducting compound, $Ca_3Ir_4Sn_{13}$, which is isostructural to $Ca_3Rh_4Sn_{13}$ [10, 15]. The dc magnetization data ($M(H)/M(T)$) in $Ca_3Ir_4Sn_{13}$ [14] revealed a long tail surviving beyond the irreversibility field/temperature (H_{irr} / T_{irr}), in contrast to the anticipated linear variation of $M(H)$ (or $M(T)$) as a function of H (or T) up to the end of the superconducting region. The experimental values of the upper critical field/superconducting transition temperature (H_{c2} / T_c) in $Ca_3Ir_4Sn_{13}$ were found to be significantly higher than those which can be ascertained following the mean field description [16] of equilibrium magnetization in a type - II superconductor. A field - temperature line, viz., (H^*,T^*), was drawn in the vortex phase diagram of $Ca_3Ir_4Sn_{13}$ [14], which runs parallel to the $H_{c2}(T)$ line. The two field-temperature lines, (H^*,T^*) and $H_{c2}(T)$, intersect the temperature axis at $T \approx 6.85$ K and $T_c \approx 7.1$ K, respectively in $Ca_3Ir_4Sn_{13}$. In an attempt to comprehend the underlying physics prevailing in the region bounded between the (H^*,T^*) and (H_{c2},T_c) lines in the vortex phase diagram of $Ca_3Ir_4Sn_{13}$ [see Fig. 7, ahead], we now present new results of dc magnetization measurements in the said region in this compound. We have observed anomalous paramagnetic signals, below T_c, in the field - cooled cool - down magnetization $M_{FCC}(T)$ measurements. These paramagnetic signals display path dependence, i.e., at a given (H,T) value, one can observe multiplicity in response. The paramagnetic peaks in $M(T)$ curves also imbibe modulations. The said features in $M_{FCC}(T)$ behaviour observed in the current investigations can be ascribed to the occurrence of multi - quanta ($L\Phi_0$, $\Phi_0 = hc/2e$, $L > 1$) vortex states at the onset of surface superconductivity and various transitions amongst multi - quanta states before the emergence of (single quantum, $L = 1$) Abrikosov flux lines. The nature of isothermal M - H scans in the close proximity of T_c lend further support to the notion

*Electronic address: santoshkumar@phy.iitb.ac.in
†Present address: Department of Physics, Indian Institute of Science Education and Research, Bhopal 462066, India.

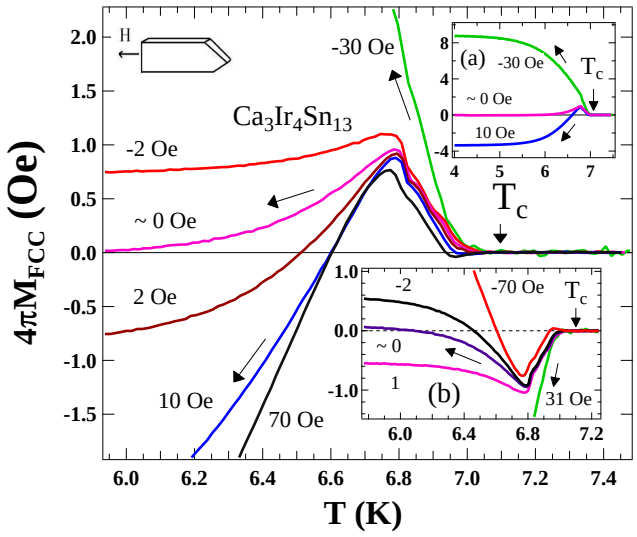

Figure 1: (Color online) Portions of $M_{FCC}(T)$ curves near T_c obtained at various magnetic field values, as indicated. Magnetic field was applied parallel to plane of the crystal. Anomalous paramagnetic signals can be noticed in the $M_{FCC}(T)$ curves for $H > 0$. The inset (a) illustrates $M_{FCC}(T)$ responses at $H = -30$ Oe, 0 Oe and 10 Oe in the range $4\,\mathrm{K} < T < 7.5\,\mathrm{K}$. The inset (b) shows the $M_{FCC}(T)$ responses recorded with a different history of the magnet (see text for details).

of multi - quanta states in the domain of surface superconductivity in the crystal of $Ca_3Ir_4Sn_{13}$ under study.

II. EXPERIMENTAL DETAILS

The single crystal specimen chosen for the present investigation is the same that was employed in Ref. [14]. The direction of magnetic field was maintained parallel to the plane of the platelet shaped sample, i.e., normal to its smallest dimension (i.e., thickness). The amplitude of vibration of the sample for the dc magnetization measurements performed using a vibrating sample magnetometer (VSM) was kept low (= 0.5 mm) for most of the runs. The magnetization was recorded in the same instrument as utilized in Ref. [14], viz., the Superconducting Quantum Interference Device Vibrating Sample Magnetometer (SQUID - VSM, Quantum Design Inc., USA).

III. RESULTS

A. Paramagnetic behaviour and the anomalous features in field-cooled magnetization measurements

Figure 1 illustrates the temperature dependences of field - cooled cool - down magnetization responses, $M_{FCC}(T)$, for various fields ($|\ H\ | < 100$ Oe), as indicated. Magnetization values were recorded while cooling the crystal from a temperature $T > T_c$ in the presence of a chosen value of applied magnetic field. Considering the presence of a remnant field appearing (when the current is set to zero) in the superconducting magnet of the SQUID - VSM, we initially attempted to estimate its magnitude and polarity by a procedure described ahead. Starting from a higher (say) positive value, we set the current in the superconducting magnet to zero. We anticipate a remnant field in the superconducting magnet, whose sign and value depend on the history of current in the magnet. We start the process of recording the magnetization data by selecting a given remnant field, whose precise value, we do not know apriori. We noticed that the $M_{FCC}(T)$ curve in the superconducting state remained positive down to the lowest temperature for $T < T_c$, which indicated that the starting remnant field was of negative polarity. We then progressively increased the applied magnetic field towards higher positive values by incrementing magnet current in small steps, and measured $M_{FCC}(T)$ responses at each selected field value. It was found that the saturated value of the $M_{FCC}(T)$ curves (see the nearly temperature - independent M_{FCC} values below about 5.5 K in the inset panel (a) of Fig. 1) crossed over to the negative side after displaying an anomalous (paramagnetic) positive peak, just below T_c (cf. main panel of Fig. 1), when the set value of applied field in magnet was $\geq +30$ Oe. We thus reckoned that the initial remnant field in the magnet was near -30 Oe in the series of M_{FCC} measurements performed, some of which are shown in Fig. 1. Keeping this estimate of remnant field in view, we arrived at the effective values of the magnetic field corresponding to each of the $M_{FCC}(T)$ curves in Fig. 1. Note that the $M_{FCC}(T)$ response for $H = -30$ Oe (cf. inset panel (a) of Fig. 1) displays a usual (i.e., diamagnetic behaviour) superconducting transition occurring at about $T = 7.1$ K (i.e., there is no apparent anomalous 'paramagnetic' magnetization feature at $H = -30$ Oe). However, on enhancing the field values from negative to positive side gradually, an anomalous positive (i.e., paramagnetic) magnetization just below T_c becomes apparent and such a behaviour was seen to persist for higher positive fields upto about $H = 1$ kOe (the magnetization curve for 1 kOe is though not displayed in Fig. 1). We also checked for the presence of the anomalous (paramagnetic) feature if the applied field is increased to higher negative values, starting from the negative value of the remanant field of the magnet. We noted that the anomalous PME like feature was not present for large negative fields. It is emphasised that the nomenclature 'positive' or 'negative' for field is arbitrary; the so called positive and negative signs of the field produced by the magnet are just the phase reversed signs. To satisfy ourselves, we repeated the record of the entire $M_{FCC}(T)$ data by beginning the process of measurements, on obtaining remanant field of positive polarity instead of negative value in the main panel of Fig. 1.

To reiterate, after setting the current (in the magnet)

once again to zero from the higher negative values (instead of higher positive values as earlier), we recorded the $M_{FCC}(T)$ data, which remained negative (i.e., diamagnetic) for $T \ll T_c$, and confirmed the remnant field to be of positive polarity. Thereafter, we gradually incremented the field from notional zero value (i.e., remenant field) to higher negative values and recorded the $M_{FCC}(T)$ data at each field value. The $M_{FCC}(T)$ responses now show the behavior, which is (nearly) a mirror image of those obtained earlier with the magnet having initial remnant field of negative polarity (see inset panel (b) of Fig. 1). The anomalous (negative) peak in $M_{FCC}(T)$ curves can now be noticed only for the negative fields, whereas no such peak (i.e., paramagnetic) feature could be observed for the positive fields. Here also, the paramagnetic nature is not seen if the applied magnetic field is increased to higher positive values. It is now instructive to note that irrespective of the magnet history, the $M_{FCC}(T)$ response initially displays a usual diamagnetic transition across the superconducting transition (cf. $M_{FCC}(T)$ curve for $H = -30$ Oe in the main panel and the inset panel (a) of Fig. 1, and for $H = 31$ Oe in the inset panel (b)) for zero current in the magnet. However, gradually reversing the sign of the field, from positive to negative or *vice-versa*, results in the above mentioned anomalous features in $M_{FCC}(T)$ plots. We are thus lead to surmise that there is no difference between the positive and negative fields in the context of the anomalous peak feature as it can be reproduced for both the signs of the field, by simply reversing the initial magnet condition (i.e., the sign of the remnant field). Such an exercise had not been carried out while reporting similar results in $Ca_3Rh_4Sn_{13}$ in Ref. [10] and perhaps had led to an erroneous surmise as if the sign of earth's field had some influence in determining the asymmetry between two signs of the applied field.

It is worthwhile to explore the possibility of encountering the anomalous paramagnetic feature in $M_{FCC}(T)$ curves (Fig. 1) in some other circumstances, say, via further change(s) in the experimental conditions. Usually, the magnitude of the remnant field gets reduced significantly by reducing the current in the magnet to zero value in an oscillating mode option of the current source. Following this alternative, the magnet current was sequentially reduced to zero in an oscillating mode from a high value of positive field: 70 kOe $\rightarrow$ 10 kOe $\rightarrow$ 1 kOe $\rightarrow$ 0 Oe (we designate this condition of remanant field as the remanant state - A). We then recorded the $M_{FCC}(T)$ responses as shown in Fig. 2(a). The remnant field in the state - A was independently reckoned to be about -5 Oe. The applied magnetic field was then increased from this remanant value to higher positive values in small steps. The paramagnetic peak in magnetization could be observed for a few field values in close proximity of the zero field, however, the peak height is substantially suppressed as compared to the corresponding values in Fig. 1. We then reversed the initial state of the magnet by setting the current such that the reduction in field in an oscillating mode goes through the sequence: -70 kOe $\rightarrow$ -10 kOe $\rightarrow$ -1 kOe $\rightarrow$ 0 Oe (designated as the remanant state - B). The remnant field was found to be $\sim +3$ Oe on this occasion. $M_{FCC}(T)$ curves were then recorded (cf. Fig. 2(b)) by increasing the current from zero value to higher negative values in small steps. It is apparent that the behavior of $M_{FCC}(T)$ curves in Fig. 2(b) almost echo the observations in Fig. 2(a) (for remnant field of negative polarity in state - A).

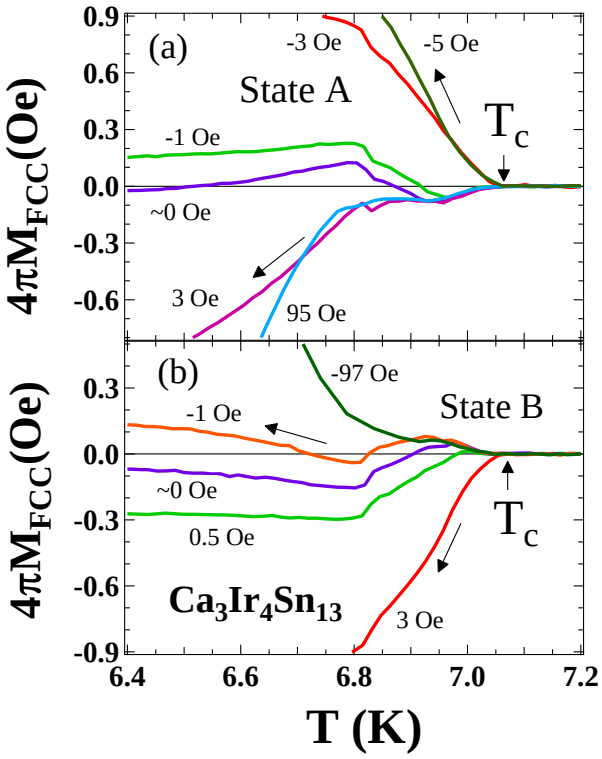

Figure 2: (Color online) $M_{FCC}(T)$ responses at various fields with the initial condition of the magnet in (a) state - A (achieved by oscillating the field and creating a small value of remnant field of negative polarity) and (b) state - B (oscillating the field and creating a small value of remnant field with positive polarity). The details of the two remanant states (A and B) have been explained in the text.

B. Metastability and non - uniqueness in M_{FCC} response

Figure 3 shows two $M_{FCC}(T)$ curves obtained for the same field value, but with opposite polarities, set in the magnet of SQUID - VSM. The panel (a) in Fig. 3 includes $M_{FCC}(T)$ for $H = \pm 10$ Oe extracted from the main panel of Fig. 1. The panel (b) in Fig. 3 contains $M_{FCC}(T)$ curves for $H = \pm 3$ Oe recorded in the state - A acquired from Fig. 2(a) and for $H = +3$ Oe obtained in the state - B from Fig. 2(b). It is well apparent from Fig. 3 that the saturated values of the $M_{FCC}(T)$

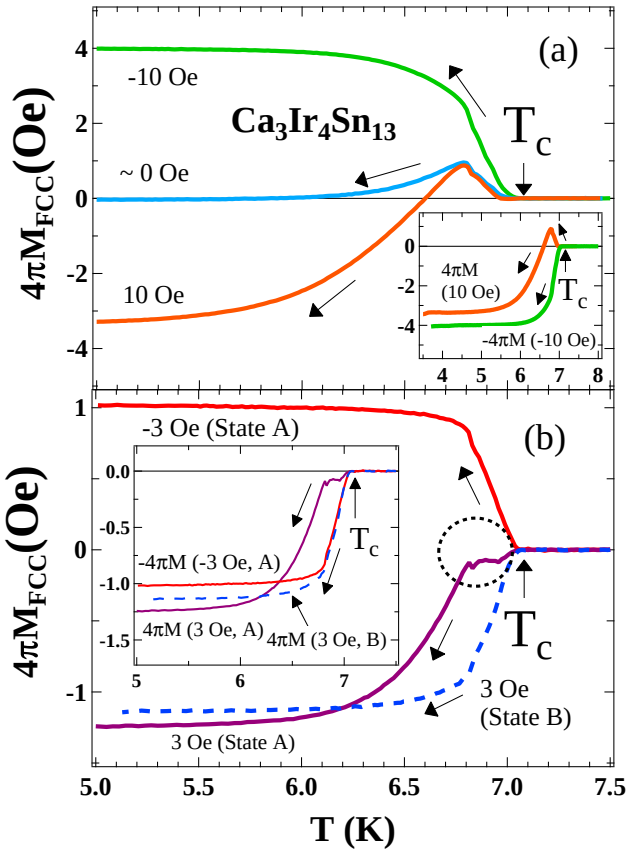

Figure 3: (Color online) (a) $M_{FCC}(T)$ for $H = 0$ Oe, ± 10 Oe. The inset panel in Fig. 3(a) compares an inverted $M_{FCC}(T)$ (i.e., $-4\pi M$ (-10 Oe)) curve at $H = -10$ Oe with $M_{FCC}(T)$ at $H = 10$ Oe; the two curves do not overlap. (b) $M_{FCC}(T)$ at $H = \pm 3$ Oe (state - A) and at $H = +3$ Oe (state - B). The inset panel in Fig. 3(b) shows an inverted $M_{FCC}(T)$ at $H = -3$ Oe (state - A) compared with $M_{FCC}(T)$ at $H = 3$ Oe of states A and B.

below $T \approx 5.5$ K are different for $\mid H \mid = 10$ Oe (cf. main panel in Fig. 3(a)) as well as for $\mid H \mid = 3$ Oe (cf. main panel in Fig. 3(b)). To elaborate this further, we show in the inset panel of Fig. 3(a), a comparison of $M_{FCC}(T)$ for $H = +10$ Oe and an inverted $M_{FCC}(T)$ curve for $H = -10$ Oe (inverted about the T - axis, i.e., $-M$ ($H = -10$ Oe)). These two curves, in the inset panel were expected to overlap, however, they showed significant differences, with a paramagnetic peak present in one case below T_c. Similar non - uniqueness in magnetization can also be observed at $\mid H \mid = 3$ Oe (see Fig. 3(b). In the inset panel of Fig. 3(b), we show an inverted $M_{FCC}(T)$ curve (see dashed curve) at $H = -3$ Oe (i.e., $-4\pi M$ (-3 Oe, A)) obtained in the state - A, which nearly overlaps with $M_{FCC}(T)$ at $H = 3$ Oe of state - B for a short window of temperature below T_c. However, the saturated $M_{FCC}(T)$ values (below about 6 K) for all three curves in the inset panel of Fig. 3(b) can be seen to be different. In addition, the $M_{FCC}(T)$ at $H = 3$ Oe obtained in the state - A also exibits undulations just below T_c which is well depicted by the encircled portion of this curve in the main panel of Fig. 3(b). However, such large undulations are not prominently seen in the other two curves ($-4\pi M$ (-3 Oe, A) and $4\pi M$ (3 Oe, B)) in Fig. 3(b).

The curious metastability and non - uniqueness observed in $M_{FCC}(T)$ data (Fig. 3) motivated us to seek information on the homogeneity of the magnetic field inside the superconducting magnet. A superconducting specimen moving in an inhomogeneous field can yield erroneous magnetization values [17], as the magnetization of the sample changes to counter the inhomogeneity in the field while moving. We decided to record the field profiles (i.e., field variation vs distance traversed on the axis of the magnet), using the flux gate option in SQUID - VSM of Quantum Design Inc., USA. Since the said flux gate option does not operate in an environment where the field value is more than $\mid 10 \mid$ Oe, the field profiles for remnant states obtained in Fig. 1 could not be traced. Hence, we prepared the magnet in the states A and B (where remanant field magnitude is expected to be less than 10 Oe). We recorded the field profiles (Fig. 4(a)) in these two states (where the remnant fields are negative and positive, respectively) as a function of distance (r) from the centre of the gradiometer coil of SQUID - VSM. We have also plotted in the inset panel of Fig. 4(a), the (parameterized) field inhomogeneity, $\triangle H/H(0)$ vs r, where $\triangle H$ ($= H(r) - H(0)$), is the difference between the field value at a given distance, r from the field value at the center of the magnet. The field inhomogeneity experienced by the sample over a scan length of 2.5 mm is found to be negligibly small ($< 10^{-2}$ Oe), as shown in the inset of Fig. 4(a). It is important to note that we had maintained the amplitude of sample vibration to be ≈ 0.5 mm for the curves plotted in Figs. 1 to 3. In addition, even for higher amplitudes (≈ 4 mm), the maximum value of the field inhomegeneity ($\triangle H/H(0)$) is about 20 mOe. This prompted us to record the $M_{FCC}(T)$ curves by varying the amplitudes of vibration in a chosen fixed field ($= 8$ Oe in Fig. 4(b)). The inset in Fig. 4(b) displays a comparison of the $M_{FCC}(T)$ curves recorded for the amplitudes of 0.5 mm and 5 mm in $H = 8$ Oe. It was interesting to find that paramagnetic peak was evident for the smallest chosen amplitude of 0.5 mm. On the other hand, the $M_{FCC}(T)$ remained diamagnetic for 5 mm amplitude in the entire temperature range, $T < T_c$. The $M_{FCC}(T)$ response in the inset panel of Fig. 4(b) shows a path dependence which resembles closely with the non - unique (path - dependent) $M_{FCC}(T)$ data shown in the inset panel of Fig. 3(a).

The main panel of Fig. 4(b) shows the evolution of the paramagnetic peak behavior when the amplitude of vibration was progressively incremented from 0.5 mm to 5 mm in steps of 0.5 mm. All the $M_{FCC}(T)$ curves traverse different paths (below T_c) as the amplitude changes. Also, the magnetization response can be seen to be oscillating in the range 6.8 K $< T < T_c$, as apparent from Fig. 4(b). It is pertinent to note that the path depen-

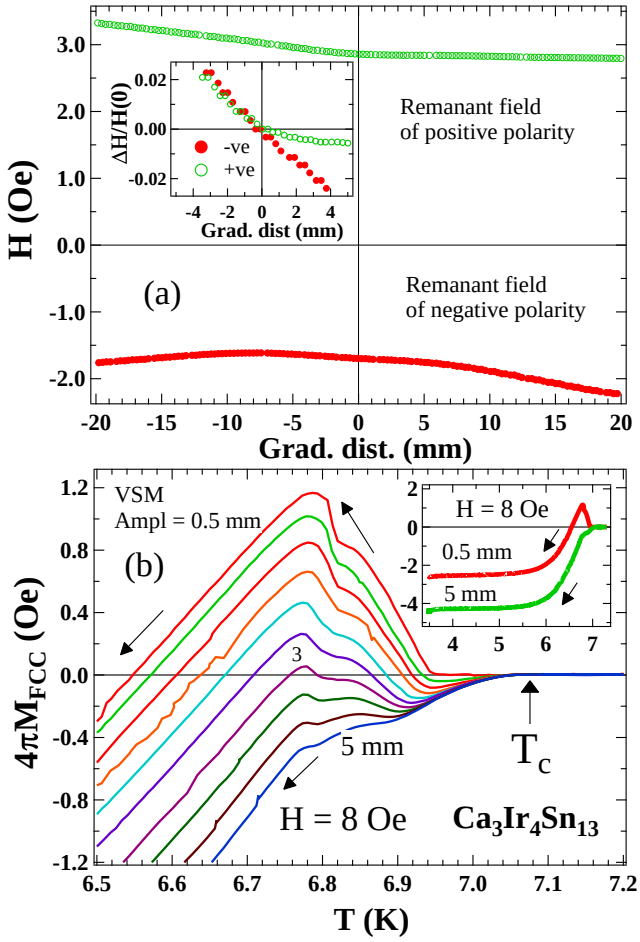

Figure 4: (Color online) (a) Remnant field profiles for state - A and state - B recorded against the distance r from centre of the gradiometer detection coil in the SQUID - VSM, Quantum Design Inc., using the flux gate option. An inset in Fig. 4(a) shows a measure of field inhomogeneity, $\triangle H/H(0)$, where $\triangle H = H(r) - H(0)$, with distance r for both the states A and B. (b) $M_{FCC}(T)$ responses in the vicinity of T_c recorded at different amplitudes of vibration (varying from 0.5 mm to 5 mm) in $H = 8$ Oe. Magnetization below T_c is path dependent and exhibits wide variations from paramagnetic to diamagnetic values. The inset in Fig. 4(b) displays $M_{FCC}(T)$ in the range, $3.5\,\mathrm{K} < T < T_c$ for the two extreme values of the amplitude of vibration, 0.5 and 5 mm.

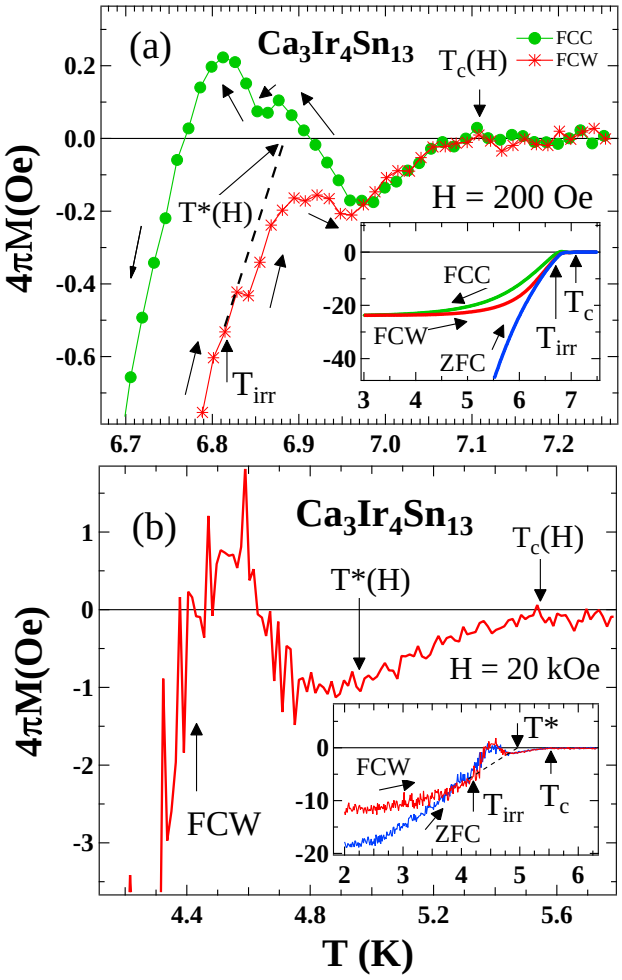

Figure 5: (Color online) (a) Expanded portions of $M_{FCW}(T)$ and $M_{FCC}(T)$ curves obtained near T_c in $H = 200$ Oe. A linear extrapolation (dashed line) of magnetization beyond the merger (at T_{irr}) of $M_{ZFC}(T)$ and $M_{FCW}(T)$ curves identifies a characteristic temperature $T^*(H)$, while $T_c(H)$ marks the onset of diamagnetism. A characteristic oscillatory behavior in $M(T)$ can be noticed below $T_c(H)$. An inset in Fig. 5(a) displays the magnetization response in all the three modes in the temperature range $3\,\mathrm{K} < T < T_c$. (b) $M_{FCW}(T)$ responses focusing attention on the oscillatory characteristic below $T_c(H)$ in $H = 20$ kOe. The inset in Fig. 5(b) shows the $M_{ZFC}(T)$ and $M_{FCW}(T)$ in $H = 20$ kOe in the temperature range, $2\,\mathrm{K} < T < 6\,\mathrm{K}$.

dence in $M_{FCC}(T)$ (inset panel of Fig. 4(b)) is not an attribute of the field inhomogeneity in the magnet of SQUID - VSM, as we have already examined in Fig. 4(a) that the $\triangle H/H(0)$ values over scan length of up to 4 mm are not sufficient to change the M values so drastically below the T_c. In addition, we also checked for any possible artefact that could arise in SQUID - VSM instrument by repeating measurements on a standard superconducting Indium sample and measured its magnetization response at a fixed chosen field in different amplitudes (from 0.5 to 8 mm) below T_c. We found no change in the magnetization values in $M_{FCC}(T)$ scans with the change in amplitude in the case of Indium sample. This assured us that the results in Fig. 4 in the case of $Ca_3Ir_4Sn_{13}$ need comprehension in terms of physics of superconductivity.

C. Oscillatory magnetization response in ($M(T)$) scans at higher fields

The inset panel of Fig. 5(a) shows the temperature variations of the zero field - cooled (M_{ZFC}), the field - cooled warm - up (M_{FCW}) and the field - cooled cool - down (M_{FCC}) magnetization responses at $H = 200$ Oe. The $M_{FCC}(T)$ and $M_{FCW}(T)$ curves, which nearly over-

lap at lower temperatures ($T < 3$ K), get separated at higher temperatures. The $M_{FCW}(T)$ and the $M_{ZFC}(T)$ curves can be seen to merge at a temperature, identified and marked as the irreversibility temperature, T_{irr} in the main panel of Fig. 5(a). According to a mean field description of type-II superconductors [16], the linear extrapolation of the reversible (i.e., equilibrium) magnetization above T_{irr} is expected to yield the superconducting transition temperature, $T_c(H)$. However, in the present case, the linear extrapolation of $M(T)$ curve above T_{irr}, identifies a characteristic temperature, $T^*(H)$, which is found to be located significantly lower than the observed superconducting transition temperature, $T_c(H)$, marking the onset of diamagnetism. The $M_{FCC}(T)$ and $M_{FCW}(T)$ curves exhibit an unusual oscillatory behavior in the vicinity of $T^*(H)$. $M_{FCC}(T)$ curve also displays paramagnetic magnetization persisting well below $T^*(H)$. The oscillatory feature is not just restricted to $M(T)$ curves at low fields, but it can also be observed at higher fields. The inset panel in Fig. 5(b) illustrates the $M_{ZFC}(T)$ and $M_{FCW}(T)$ curves recorded in $H = 20$ kOe. The irreversibility temperature, T_{irr} and the characteristic temperature, $T^*(H)$ are identified and marked in the inset of Fig. 5(b). An expanded plot of $M_{FCW}(T)$ in the vicinity of T_c (main panel of Fig. 5(b)) shows the oscillatory magnetization response in $H = 20$ kOe. In addition, the $M_{FCW}(T)$ curve in $H = 20$ kOe is also paramagnetic below $T^*(H)$, like the $M_{FCC}(T)$ curve in $H = 200$ Oe, as is apparent from a comparison of respective curves in the main panels of Fig. 5(a) and 5(b).

D. Metastable magnetization response and evidence for multi-quanta ($L > 1$) states

The region close to T_c has further been explored via the isothermal ($M(H)$) measurements. Figure 6 shows the M–H responses at $T = 6.85$ K (panels (a) and (b)), 6.90 K (panels (c) and (d)) and 6.95 K (panels (e) and (f)). The $M(H)$ curve at $T \approx 7.1$ K (normal state) is also shown in panels (a), (c) and (e) for comparison. In each case, the sample was first cooled in a field H ($> H_{c2}(T)$) from a temperature $T > T_c$ to the desired temperature. The magnetization was then recorded while ramping the field to higher negative values and then back to higher positive values. At $T \approx 7.10$ K, the M–H curve remains linear in the entire field range as expected for the normal state ($T_c \approx 7.1$ K) of a superconductor. Even though the M–H curve at $T = 6.85$ K in Fig. 6(a) appears, at first sight, to be typical of a type-II superconductor, some anomaly can be clearly seen in the magnified view near $H = 20$ Oe (see Fig. 6(b)). There are unusual dips (see encircled regions in Fig. 6(b)) in magnetization near $H \approx 0$, which are not expected for a type-II superconductor. Moreover, there is a sharp positive peak in the magnetization at $H \approx 0$ Oe and the magnetization response is also found to be asymmetric about the M-axis,

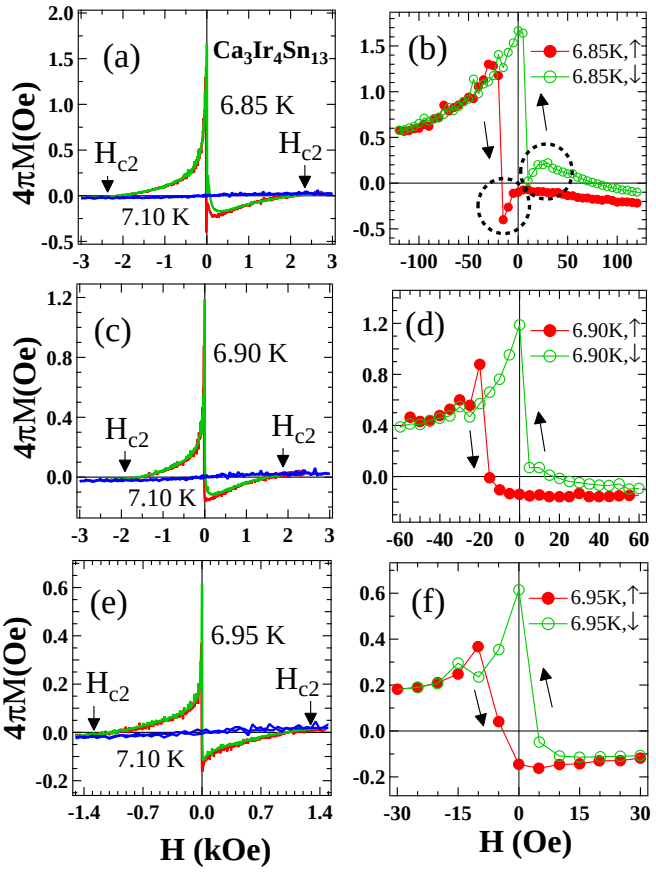

Figure 6: (Color online) Isothermal $M(H)$ scans recorded at (a) $T = 6.85$ K, (c) $T = 6.90$ K and (e) $T = 6.95$ K. $M(H)$ curve at $T = 7.1$ K (normal state) is also shown in all three panels. Expanded portions of $M(H)$ curves near $H = 0$ are displayed in the right panels, (b) (6.85 K), (d) (6.90 K) and (f) (6.95 K). Features near zero field, viz., unusual dips (encircled in panel (b)), a positive magnetization and an apparent asymmetry in $M(H)$ for opposite signs of fields (panel (b), (d) and (f)) do not conform to typical type-II superconducting behavior.

as evident in Fig. 6(b). Note that the asymmetry in magnetization about M-axis in the M–H scan reminds of the asymmetry observed earlier (see, for example, Fig. 3) in the temperature variations of the field-cooled magnetization ($M_{FCC}(T)$) for the opposite polarities of the magnetic field. At a higher temperature, $T = 6.90$ K (cf. Fig. 6(c)), one can notice that the asymmetry in the M–H curve persists, however, unlike the situation in Fig. 6(b), there is no fingerprint of the dip like feature near $H \sim 10$ Oe (see the magnified view in Fig. 6(d)). The dips observed in Fig. 6(b) have now morphed into a huge magnetization near zero field at $T = 6.90$ K even though the system is still in the superconducting state. Similarly at $T = 6.95$ K (Fig. 6(e)), the positive peak in magnetization at $H \approx 0$ and a nominal hysteresis in the M–H curve (cf. Fig. 6(f)) could be seen, which potray a completely different picture than that for a usual type-II superconducting behavior.

IV. DISCUSSION: H–T PHASE SPACE OF SURFACE SUPERCONDUCTIVITY

It is tempting to associate the anomalous features observed in Figs. 1 to 6, with some theoretical findings. The observation of paramagnetic magnetization in the superconducting state of a conventional superconductor is generally known to be an attribute of the compression of trapped flux [1, 3, 6] within the bulk of a sample that leads to giant vortex states with multiple flux quanta ($L \gg 1$). The self-consistent solutions [3, 6, 18] of the G - L equations for certain geometries and various (mesoscopic) dimensions of superconducting specimen yield multi - quanta states ($L \gg 1$) at the onset of surface superconductivity [13]. These multi - quanta states ($L \gg 1$) tend to transform into pinned (single quantum, $L = 1$) Abrikosov lattice on lowering the temperature (in a constant field) across the notional second critical field, $H_{c2}(T)$ line of the H–T space. However, such a transformation can follow a large variety of paths [6] involving several internal transitions amongst the multi-quanta states. Each of these multi - quanta states has a unique $M(H)$ loop associated with it such that the magnetic response is diamagnetic at higher fields, which crosses over to paramagnetic values at lower fields (see, for instance, Figs. 2 and 3 in Ref. [6] and Figs. 16, 17 and 23 in Ref. [18]). If the superconducting state created (below T_c) gets stuck in a certain $L\,(> 1)$ state in a metastable manner, the magnetization state initially ought to be diamagnetic (see Fig. 2(b) in Ref. [6]), which then crosses over to paramagnetic values (along the $M(H)$ curve of a given L state) as the temperature is swept down in a constant field. The $M_{FCC}(T)$ curves below 3 mm amplitude in Fig. 4(b) and those of Fig. 1 in a sense illustrate such a behaviour.

Since there is a specific field - temperature domain of each $L > 1$ state [6, 18], changes in the H or T values can also bring transitions [6] from one L state into another L value. Such transitions are generally accompanied with abrupt (jumps) changes in magnetization [6, 19]. The undulations overriding the PME and the oscillatory response in Figs. 1 to 5 could be viewed as elucidation of such transitions. According to Zharkov's results [6], the magnetization signal will remain diamagnetic if transitions continue to happen involving the neighbouring states following the lowest free energy criterion (see Fig. 2(b) in Ref. [6] for transitions between L and $L \pm 1$ states). However, if one allows for metastability and for transitions to happen between different metastable states, it can lead to a complex magnetization response such that, magnetization signal can change from a given paramagnetic/diamagnetic value to higher/lower value (see Fig. 3(b) in Ref. [6]).

Features emanating from the $M_{FCC}(T)$ curves of Fig. 4(b) elucidate a wide variety, from diamagnetic to paramagnetic values (induced by the change in vibration amplitude) in the $M_{FCC}(T)$ responses below T_c, which can be associated with the metastable nature arising out

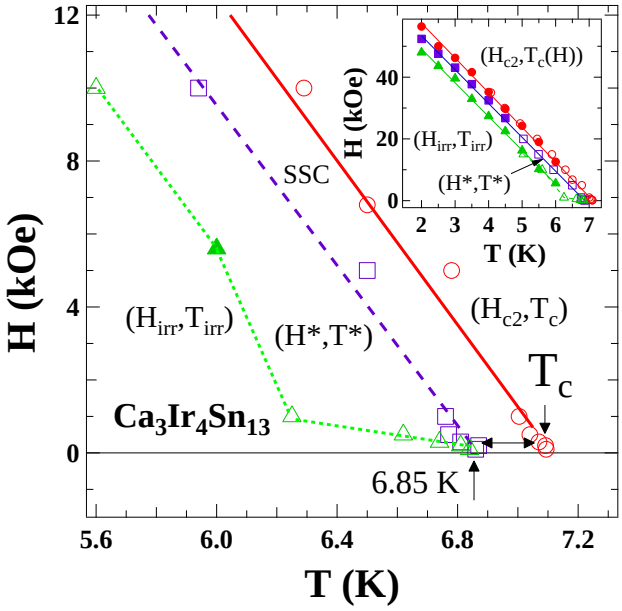

Figure 7: (Color online) A portion of the H–T phase diagram for $Ca_3Ir_4Sn_{13}$ (extracted from our earlier report, Ref. [14]). It comprises an irreversibility (H_{irr},T_{irr}) line, the characteristic field/temperature (H^*,T^*) line and the upper critical field (H_{c2},T_c) line as obtained from Fig. 4. The inset in Fig. 6 displays the complete phase diagram. The phase - space region bounded by (H^*,T^*) and (H_{c2},T_c) lines has been surmised to be the region of surface superconductivity.

of a variety in the multi - quanta states in the domain of surface superconductivity. The non - uniqueness in magnetization is also well apparent from Fig. 3 wherein the $M_{FCC}(T)$ is recorded at constant amplitude ($= 0.5$ mm) for opposite polarities of a given H. Since the non - uniqueness in $M_{FCC}(T)$ persists even for lower temperatures as the saturated $M_{FCC}(T)$ values are significantly different in the inset panels of Figs. 3(a), 3(b) and Fig. 4(b), one may also argue that a non - unique coexistence of multi - quanta ($L > 1$) and single quantum ($L = 1$) states is being witnessed far below T_c.

Another interesting facet of Zharkov's findings [6] derives from the free energy plots of various L states (see Fig. 3(c) in Ref. [6]), which predicts a short temperature window just below T_c, where the single quantum (Abrikosov) state does not exist. Consistent with this prediction, the $M(H)$ loops recorded in the proximity of T_c (cf. Fig. 6) in $Ca_3Ir_4Sn_{13}$ display anomalous features which are not anticipated for a pinned type - II superconductor. The lack of evidence for (pinned) Abrikosov vortex state ($L = 1$) above 6.95 K in $Ca_3Ir_4Sn_{13}$ presumably echo the predictions of Zharkov [6].

From the viewpoint of surface superconductivity, we are now inclined to reconsider the field - temperature (H–T) phase - space of $Ca_3Ir_4Sn_{13}$ reported in our earlier investigation [14], which is reproduced in Fig. 7. The (H^*, T^*) line, as obtained from Fig. 5, in this phase di-

agram can now be surmised as a crossover regime between the bulk and the surface superconductivity. The (H_{c2},$T_c(H)$) line in Fig. 7 can be surmised as the third critical field line. The region enclosed between the (H^*,T^*) and (H_{c2},$T_c(H)$) lines is identified as the region where surface superconductivity (SSC) dominates. As stated above, the H–T region bounded by the interval 6.85 K $< T < T_c$ does not imbibe fingerprints of Abrikosov flux line lattice; it is only below $T \approx 6.85$ K, the mean - field description is expected to be applicable in $Ca_3Ir_4Sn_{13}$. In this context, we believe that the (H^*,T^*) line meeting the T - axis at $T \approx 6.85$ K (surmised as bulk superconducting transition) is reasonable. Across the interval $T^* < T < T_c$, the $M(T)$ (Fig. 5) and the M–H (Fig. 6) responses reflect the metastable nature of the multi - quanta ($L > 1$) vortex states occurring in the domain of surface superconductivity.

V. SUMMARY

We have investigated a weakly-pinned single crystal of a low T_c superconducting compound, $Ca_3Ir_4Sn_{13}$ via dc magnetization measurements. Recently we explored [14] the pinning behaviour, order - disorder transitions in the vortex matter and the vortex phase diagram in this compound. The said vortex phase diagram of $Ca_3Ir_4Sn_{13}$ in our previous report [14] had left some issues unresolved, for example, a non - linear behaviour in the reversible magetization response ($M(T)/M(H)$) was observed close to the $T_c(H)$ line. The low field $M_{FCC}(T)$ data in the present report reveals some intriguing features, viz., anomalous paramagnetic signals, a rich multiplicity or non - uniqueness in magnetization ranging from diamagnetic to paramagnetic values, oscillatory magnetization response below T_c, etc. These novel features have been associated with the occurrence of multi - quanta states in the domain of surface superconductivity and the metastability effects associated due to the transitions amongst various multi - quanta states ($L > 1$) in this compound. The isothermal M–H responses in the temperature range 6.85 K$< T < T_c$ (Fig. 6), corroborate further the notion of multi - quanta ($L > 1$) vortex states in the realm of surface superconductivity.

The paramagnetic magnetization ($M_{FCC}(T)$) observed in $Ca_3Ir_4Sn_{13}$ is ascribed to the multi - quanta states ($L > 1$) occurring in the domain of surface superconductivity, even though, other explanations behind the paramagnetic nature cannot be ruled out. About a decade ago, such a behavior was theoretically anticipated using the G - L theory for specific situations [3, 6, 18]. We believe that the present work has provided some experimental evidences rationalizing the predictions of those theoretical works [3, 6, 18].

Acknowledgments

Santosh Kumar would like to thank the Council of Scientific and Industrial Research, India for grant of the Senior Research Fellowship.

[1] A. E. Koshelev and A. I. Larkin, Phys. Rev. B 52 (1995) 13559.
[2] A.E. Khalil, Phys. Rev. B 55 (1997) 6625.
[3] V. V. Moshchalkov, X. G. Qui, and V. Bruyndoncz, Phys. Rev. B 55 (1997) 11793.
[4] L. Pust, L. E. Wenger, M. R. Koblischka, Phys. Rev. B 58 (1998) 14191.
[5] A. K. Geim, S. V. Dubonos, J. G. S. Lok, M. Henini and J. C. Maan, Nature (London) 396 (1998) 144.
[6] G. F. Zharkov, Phys. Rev. B 63 (2001) 214502.
[7] M. A. Lopez de la Torre, V. Pena, Z. Sefrioui, D. Arias, C. Leon, J. Santamaria, J. L. Martinez, Phys. Rev. B 73 (2006) 052503.
[8] P. Das, C. V. Tomy, S. S. Banerjee, H. Takeya, S. Ramakrishnan and A. K. Grover, Phys. Rev. B 78 (2008) 214504.
[9] M. J. R. Sandim, D. Stamopoulos, L. Ghivelder, S. C. V. Lim, A. D. Rollett, J. Supercond. Nov. Mag. 23 (2010) 1533.
[10] P. D. Kulkarni, S. S. Banerjee, C. V. Tomy, G. Balakrishnan, D. McK. Paul, S. Ramakrishnan, and A. K. Grover, Phys. Rev. B 84 (2011) 014501.
[11] Santosh Kumar, A.D. Thakur, R.P. Singh, A. Thamizhavel, C.V. Tomy and A.K. Grover, AIP Conf. Series 1447 (2012) 909-910.
[12] U. Vaidya, P.D. Kulkarni, H. Takeya, S. Ramakrishnan and A.K. Grover, AIP Conf. Series 1447 (2012) 903-904.
[13] D. Saint-James and P. G. de Gennes, Phys. Lett. 7 (1963) 306.
[14] Santosh Kumar, Ravi P. Singh, A. Thamizhavel, C. V. Tomy and A. K. Grover, accepted in Physica C, arXiv:1408.1525v1 [cond-mat.supr-con], 7 Aug 2014.
[15] J. P. Remeika, G. P. Espinosa, A. S. Cooper, H. Barz, J. M. Rowell, D. B. McWhan, J. M. Vanderberg, D. E. Moncton, Z. Fisk, L. D. Woolf, H. C. Hamaker, M. B. Maple, G. Shirane and W. Thomlinson, Solid State Commun. 34 (1980) 923.
[16] M. Tinkham, Introduction to Superconductivity, 2nd ed., McGraw-Hill International Edition (1996).
[17] G. Ravikumar et al., Physica C 298 (1998) 122-132.
[18] V. A. Schweigert and F. M. Peeters, Phys. Rev. B 57 (1998) 13817.
[19] A. Bezryadin, A. Buzdin, B. Pannetier, Phys. Rev. B 51 (1995) 3718.